Filamentary star formation and the role of magnetic fields on various scales with SALTUS–B-BOP

Often ignored, strong, organized magnetic fields, in rough equipartition with the turbulent and cosmic ray energy densities, have been detected in the ISM of a large number of galaxies out to $z = 2$ (e.g. Beck, 2015). Recent cosmological MHD simulations of structure formation in the Universe suggest that magnetic-field strengths comparable to those measured in nearby galaxies ($\lesssim 10\,\mu$G) can be quickly built up in high-redshift galaxies (in $<< 1$ Gyr), through the dynamo amplification of initially weak seed fields (e.g. Rieder & Teyssier, 2017). Magnetic fields are therefore expected to play a dynamically important role in the formation of giant molecular clouds (GMCs) on kpc scales within galaxies (e.g. Inoue & Inutsuka, 2012) and in the formation of filamentary structures leading to individual star formation on ∼1–10 pc scales within GMCs (e.g. Inoue et al., 2018, Inutsuka et al., 2015, see § 1 below). On dense core (≤ 0.1 pc) scales, the magnetic field and angular momentum of most protostellar systems are likely inherited from the processes of filament formation and fragmentation (cf. Misugi et al., 2019). On even smaller (< 0.01 pc or < 2000 au) scales, magnetic fields are essential to solve the angular momentum problem of star formation, generate protostellar outflows, and control the formation of protoplanetary disks (Li et al., 2014). In this context, high-dynamic-range mapping observations of linearly-polarized continuum emission from magnetically-aligned dust grains at far-IR and submm wavelengths with **SALTUS–B-BOP can provide a unique tool for characterizing the role of magnetic fields from GMC to protostellar scales** (§ 4).

1. Insights from *Herschel* and *Planck*: A filament paradigm for star formation

The *Herschel* mission has led to spectacular advances in our knowledge of the texture of the cold ISM and its link with star formation. *Herschel* imaging surveys have established the ubiquity of interstellar filaments on almost all length scales (∼ 0.5 to ∼ 100 pc) in the molecular clouds of the Galaxy and shown that this filamentary structure likely plays a key role in the star formation process (e.g. André et al., 2010, Hill et al., 2011, Molinari et al., 2010, Schisano et al., 2014). *Herschel* observations of nearby molecular clouds indicate that interstellar filaments have a characteristic inner width ∼ 0.1 pc (Arzoumanian et al., 2011, 2019), and that prestellar cores and protostars form primarily in dense, gravitationally "supercritical" filaments above a critical threshold $\sim 16\,M_\odot/\mathrm{pc}$ in mass per unit length, equivalent to a critical threshold $\sim 160\,M_\odot/\mathrm{pc}^2$ ($A_V \sim 8$) in column density or $n_{H2} \sim 2 \times 10^4\,\mathrm{cm}^{-3}$ in volume density (Könyves et al., 2015). These *Herschel* results support a filament paradigm for star formation in two main steps (e.g. André et al., 2014, Inutsuka et al., 2015): First, multiple large-scale compressions of interstellar material in supersonic magneto-hydrodynamic (MHD) flows generate a cobweb of ∼ 0.1 pc-wide filaments in the ISM; second, the densest filaments fragment into prestellar cores (and subsequently protostars) by gravitational instability above the critical mass per unit length of nearly isothermal, cylinder-like filaments (see Fig. 1). A merit of this paradigm is that it may account for at least part of the prestellar core mass function (CMF) and by extension part of the stellar IMF (André et al., 2019, Lee et al., 2017). **In this paradigm, the origin of the IMF is deterministic and directly linked to the prestellar CMF and filament line mass function (FLMF).** It has also been argued that **the filamentary structure may help to regulate the SF efficiency in dense molecular gas** (André et al., 2014), and may be responsible for a quasi-universal SF law in the dense giant molecular clouds (GMCs) of galaxies (Lada et al., 2012, Shimajiri et al., 2017). Improving our understanding of the physics and detailed magnetic properties of **molecular filaments** is thus of paramount importance as the latter **are representative of the initial conditions for star formation and the IMF within GMCs**.

In parallel to *Herschel*, the *Planck* mission has led to major advances in our knowledge of the geometry of the magnetic field on large scales in the Galactic ISM. The first all-sky maps of dust polarization provided by *Planck* at 850 μm have revealed a highly organized magnetic field structure on $\gtrsim$ 1–10 pc scales in Galactic interstellar clouds (Planck int. res. XXXV, 2016, see Fig. 1a). The large-scale magnetic field tends to be aligned with low-density filamentary structures with subcritical line masses and perpendicular to dense star-forming filaments with supercritical line masses (Planck int. res. XXXII, 2016, Planck int. res. XXXV, 2016, see Fig. 1b). There is also a hint from *Planck* polarization observations of the nearest clouds and ALMA observations of high-mass infrared dark clouds (IRDCs) that the direction of the magnetic field may change *within* dense filaments from

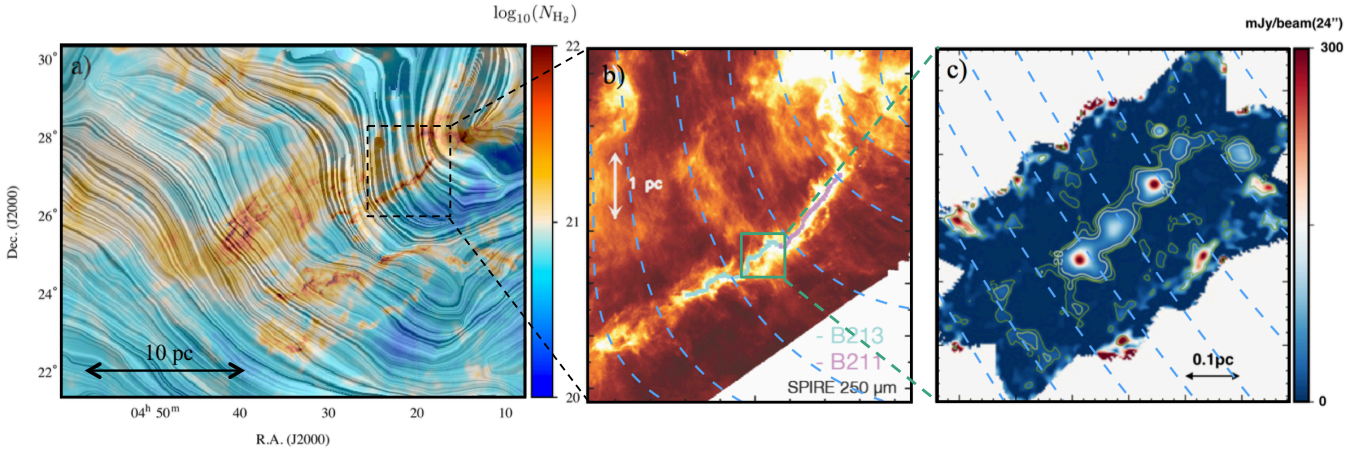

Figure 1: **(a)** Multi-resolution column density map of the Taurus molecular cloud as derived from high-resolution (18″–36″ HPBW) *Herschel* Gould Belt survey data and low-resolution (5′ HPBW) *Planck* data. The superimposed "drapery" pattern traces the B-field orientation projected on the plane of the sky (POS), as inferred from *Planck* polarization data at 850 μm (Planck int. res. XXXV, 2016). **(b)** *Herschel* 250 μm dust continuum image of the Taurus B211/B213 filament (Marsh et al., 2016, Palmeirim et al., 2013). The blue dashed curves trace the POS B-field orientation from *Planck* (Planck int. res. XXXV, 2016). **(c)** IRAM/NIKA1 1.2 mm continuum image of the central part of the *Herschel* field shown in (b) (effective HPBW resolution ∼20″), showing a chain of four equally-spaced dense cores along the B211-3 filament (from Bracco et al., 2017). SALTUS–B-BOP can image the B-field lines at a factor > 100 better resolution than *Planck* over the entire Taurus cloud (cf. panel **a**), probing scales from < 1000 a.u. to > 10 pc.

nearly perpendicular in the ambient cloud to more parallel in the filament interior (Dall'Olio et al., 2019, Planck int. res. XXXIII, 2016). These findings suggest that **magnetic fields play a key role in the formation and evolution of filamentary structures** in interstellar clouds, supporting the view that dense molecular filaments form by accumulation of interstellar matter along field lines. **The low resolution of *Planck* polarization data** (10′ at best or ∼0.4 pc in nearby clouds) **is however insufficient to probe the organization of field lines in the ∼ 0.1 pc interior of filaments**, corresponding both to the characteristic transverse scale of filaments (Arzoumanian et al., 2011, 2019) and to the scale at which fragmentation into prestellar cores occurs (cf. Tafalla & Hacar, 2015). Consequently, **the geometry of the magnetic field *within* interstellar filaments and its effects on fragmentation and star formation are essentially unknown at present**.

2. Role of magnetic fields in the formation and evolution of molecular filaments

Magnetic fields are likely central to the explanation of how dense molecular filaments can maintain a roughly constant ∼0.1 pc inner width while evolving and forming stars. One plausible evolutionary scenario, consistent with existing observations, is that star-forming filaments accrete ambient cloud material along field lines through a network of magnetically-dominated striations (e.g. Cox et al., 2016, Palmeirim et al., 2013). Accretion-driven MHD waves may then generate a system of velocity-coherent fibers within dense filaments (Arzoumanian et al., 2013, Hacar et al., 2013, Hennebelle & André, 2013, cf. Fig. 2) and the corresponding organization of magnetic field lines may play a central role in accounting for the roughly constant ∼ 0.1 pc inner width of star-forming filaments. Constraining this process further is key to understanding star formation itself, since filaments with supercritical masses per unit length would otherwise undergo rapid radial contraction with time, effectively preventing fragmentation into solar-type protostellar cores (e.g. Inutsuka & Miyama, 1997). Information on the geometry of magnetic field lines *within* star-forming filaments at $A_V > 8$ is crucially needed, and can be obtained through 70–350 μm dust polarimetric imaging with SALTUS–B-BOP. Both high angular resolution and high spatial dynamic range are needed to resolve the 0.1 pc scale by a factor ∼ 3–10 on one hand and to probe spatial scales from > 10 pc in the low-density striations of the ambient cloud (see Fig. 1), down to ∼0.01–0.03 pc for the fibers

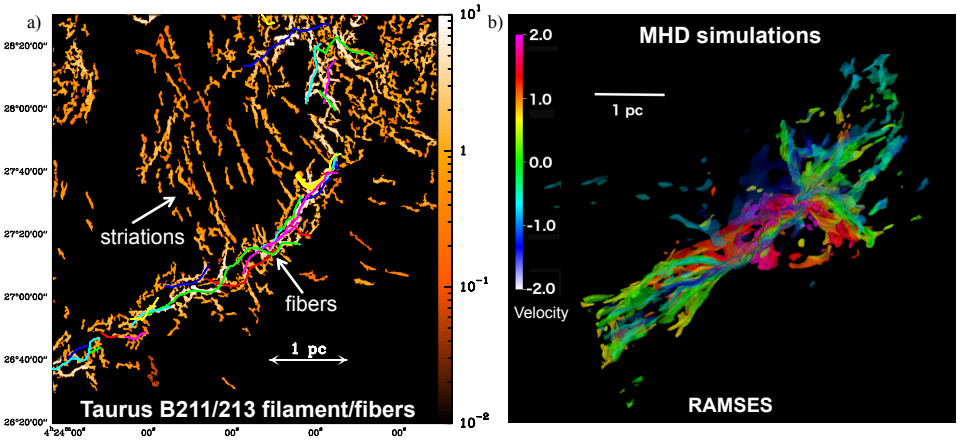

Figure 2: **(a)** Fine (column) density structure of the B211/B213 filament based on a filtered version of the *Herschel* 250 μm image of (Palmeirim et al., 2013) using the algorithm *getfilaments* (Men'shchikov, 2013). In this view, all transverse angular scales larger than 72″ (or ~ 0.05 pc) were filtered out to enhance the contrast of the small-scale structure. The color scale is in MJy/sr at 250 μm. The colored curves display the velocity-coherent fibers independently identified by (Hacar et al., 2013) using $N_2H^+/C^{18}O$ observations. **(b)** MHD simulation of a collapsing/accreting filament performed by E. Ntormousi & P. Hennebelle with the AMR code RAMSES. Velocities along the z axis (in km/s) after one free-fall time (~ 0.9 Myr) are coded by colors. For clarity, only the dense gas with $n_{H_2} > 10^4\,\mathrm{cm}^{-3}$ is shown.

of dense filaments (see Fig. 2). In nearby Galactic regions (at $d \sim 0.15$–1.5 kpc), this corresponds to angular scales from > 5 deg or more down to $\sim 5''$ or less.

A specific objective of SALTUS–B-BOP observations will be to test the hypothesis, tentatively suggested by recent *Planck* and ALMA polarization results (Dall'Olio et al., 2019, Planck int. res. XXXIII, 2016) that the magnetic field becomes nearly parallel to the long axis of star-forming filaments in their dense interiors at scales < 0.1 pc, due to, e.g., gravitational compression (see Fig. 3). Should this prove to be the case, it could explain both how dense filaments maintain a roughly constant ~ 0.1 pc width while evolving (cf. Seifried & Walch, 2015) and why the observed spacing of prestellar cores along the filaments is significantly shorter than the characteristic fragmentation scale of $4\times$ the filament diameter expected in the case of non-magnetized nearly isothermal gas cylinders (e.g. Inutsuka & Miyama, 1992, Kainulainen et al., 2017, Nakamura et al., 1993).

As a **practical illustration of what could be achieved with SALTUS–B-BOP**, a reference polarimetric imaging survey would be to map, in Stokes I, Q, U at 70 μm or 100 μm, 200 μm, and 350 μm, a similar $\sim 100\,\mathrm{deg}^2$ area in nearby interstellar clouds at $d \lesssim 3$ kpc to that imaged by *Herschel* in Stokes I at 70–500 μm as part of the Gould Belt, HOBYS, and Hi-GAL surveys (André et al., 2010, Molinari et al., 2010, Motte et al., 2010). (Adopting the performance parameters given in the "SALTUS/B-BOP Fact Sheet" and an observing time of ~ 10 hr per square degree, such a survey would reach a typical signal-to-noise ratio of ~ 5 or more in Q, U intensity at 200 μm and 350 μm over the entire molecular part of the clouds ($A_V \gtrsim 1$) at the full SALTUS resolution, assuming a typical polarization fraction $p \sim 5\%$ and a typical dust temperature $T_d \sim 17$ K at $A_V \sim 1$, and $p \sim 3\%$, $T_d \sim 10$–13 K in the dense inner regions ($A_V \gtrsim 10$). The entire survey of $\sim 100\,\mathrm{deg}^2$ would require ~ 1000 hr of observing time. It would provide key information on the magnetic field geometry for thousands of filamentary structures spanning more than ~ 2 orders of magnitude in column density from low-density subcritical molecular filaments at $A_V \sim 1$ to star-forming supercritical filaments in the dense inner parts of molecular clouds at $A_V \gtrsim 100$.

3. Role of magnetic fields in forming stellar systems and the first planetesimal seeds

Along filaments in molecular clouds, protostellar dense cores are the "seeds" where the gravitational force proceeds to form stars. The dust characteristics, the magnetic field, and the gas

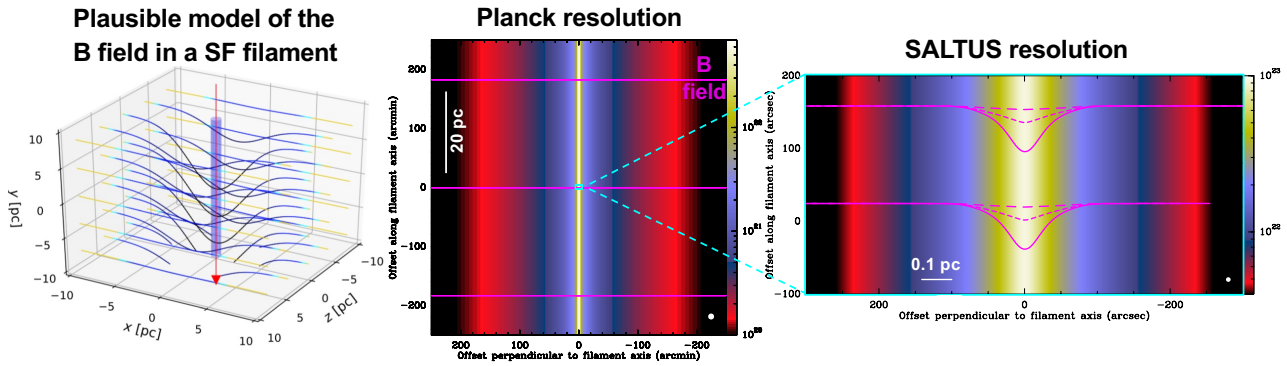

Figure 3: **(a)** 3D view of a plausible model of the magnetic field structure within a star-forming filament. **(c)** Synthetic column density map and B-field geometry derived for this model filament at the *Planck* resolution, assuming a distance $d = 500$ pc for the filament. **(c)** Synthetic column density map and B-field geometry derived for the same model filament from SALTUS–B-BOP data at 100–350 μm. The various curves represent B-field lines projected in the plane of sky as derived from SALTUS–B-BOP observations at 100 μm (long-dashed), 200 μm (short-dashed), and 350 μm (solid). Due to the dust temperature gradient inside the filament, and weighted integration of density/polarization along the line of sight, **observations at different wavelengths effectively probe the B-field at different depths in the filament, offering the prospect of partial tomographic reconstructions of the B-field geometry**.

dynamics of protostellar cores all bear a relationship to the properties of the parent filaments. However, it is debated whether the angular momentum of the circumstellar gas, ultimately responsible for the formation of protoplanetary disks, is inherited from the large-scale compressive and shearing motions at the origin of the parent filaments (e.g. Misugi et al., 2019, Pudritz & Kevlahan, 2013) or from more localized, anisotropic collapse motions inside the cores themselves (Verliat et al., 2020). Similar questions still stand regarding the changes in magnetic field topology and strength, as well as dust evolution, from filament scales down to disk scales.

All protostellar cores are magnetized to some level: current observations of the magnetic field at core scales are scarce but suggest that in most solar-type protostars, the B-field is remarkably well organized on small scales since a main component is successfully observed in almost all Class 0 protostars (Galametz et al., 2020). Some indications have also been found, in small samples ($\sim$ 20 objects), that the topology of the B-field at thousands au scales may be linked to the distribution of angular momentum in solar-type protostellar cores, and hence that the magnetic field may be of paramount importance in the formation process of multiple stellar systems and protoplanetary disks around solar-type stars (see Galametz et al. 2020, 2018, Segura-Cox et al. 2018, Yen et al. 2021). These observations and their detailed comparison to models point toward a large fraction of objects being under strong field conditions at core scales (e.g., Girart et al., 2006, Kwon et al., 2019, Maury et al., 2018), while in more resolved studies and/or more massive cores (e.g., Ching et al. 2017, Girart et al. 2013, Hull et al. 2017) the B-field shows a more complex morphology. Moreover, there is a debate regarding the regulating role of the B-field to control the level of sub-fragmentation driving the formation of massive binaries, during protostellar collapse, in massive protostars. In the massive IRDC G14.225-0.506, for example, a low-level of sub-fragmentation is observed in the northern hub which has a more regular (and presumably stronger) magnetic field than the more highly fragmented southern hub (Busquet et al., 2016, 2013), although statistical studies suggest this correlation may be weak (Palau et al. 2021). Current studies are however limited: observing much larger, complete samples of protostars is crucially needed before definite conclusions can be drawn about the dynamical role of magnetic fields at core scales for the building of star-disk systems.

The angular resolution and surface brightness dynamic range of SALTUS–B-BOP will make it possible to resolve most $\sim$1000–20000 au protostellar cores in nearby star-forming regions out to $\sim$1 kpc. A wide-field SALTUS–B-BOP survey of all nearby protostellar populations as envisaged in § 2 ($\sim$ 2 hr per square degree) will map dust polarized emission (fraction $> 1\%$) at core scales with

signal-to-noise ratio > 7, in complete populations of $\gtrsim 1000$ protostars (Class 0 and Class I) and their parent cloud/environment, from massive protostellar cores down to the low-mass progenitors of solar-type stars. SALTUS–B-BOP will provide information on the geometry of magnetic field lines and properties of the dust producing the polarized emission across the full protostellar core mass distribution, probing different behaviors in different mass regimes, and potentially as a function of environment in different star-forming regions. In contrast, current millimeter/submillimeter polarimetric instruments, such as SCUBA2-POL, NIKA2-POL, SOFIA/HAWC+, or BLAST-TNG (cf. § 4) are limited to the subset of the ∼50-100 brightest cores, and without the important context provided by the magnetic field information in the parental clouds.

SALTUS will also directly address the question of grain growth leading to the formation of planetesimals in a magnetized star formation scenario. Indeed, magnetic fields may not only alter the properties of young planet-forming disks, but may also significantly change our current understanding of dust evolution in circumstellar environments. Recent studies have found hints that circumstellar dust at core scales, directly involved in feeding planet-forming disks, may be very different from ISM dust (Galametz et al., 2019). Measurements of the spectral index of polarized thermal dust emission is a new powerful tool to investigate dust properties (Guillet et al., 2020, Valdivia et al., 2019). Spatially-resolved SALTUS observations of the submm polarized spectral index in large samples of protostellar cores will enable to characterize the pristine properties of planet-forming material, such as dust grain sizes in protostellar envelopes, thereby setting crucial constraints on the timescales for the formation of planetary bodies around stars like our Sun.

The magnetic field properties and dust properties found with SALTUS–B-BOP at dense core scales can be compared with the properties observed with interferometers at disk scales to build correlation diagrams (cf. Galametz et al., 2020). In this way, SALTUS–B-BOP observations can test the hypothesis, tentatively suggested by current studies, that magnetic fields may regulate the properties of planet-forming disks, and stellar systems during the main accretion phase.

4. Key advantages of SALTUS over other polarimetric facilities

Far-IR/submm polarimetric imaging from space with SALTUS–B-BOP will have unique advantages, especially in terms of spatial dynamic range *and* surface brightness dynamic range. Studying the multi-scale physics of star formation within molecular filaments requires a spatial dynamic range of ~ 1000 or more to simultaneously probe scales $> 10\,\mathrm{pc}$ in the parent clouds down to $\sim 0.01\,\mathrm{pc}$ in the interior of star-forming filaments (corresponding to angular scales from $\sim 4''$ to $> 5\,\mathrm{deg}$ in the nearest molecular clouds at $d < 1.5\,\mathrm{kpc}$ – see Fig. 1). Such a high spatial dynamic range was routinely achieved with *Herschel* in non-polarized imaging, but has never been obtained in ground-based submm continuum observations. It can be achieved with SALTUS–B-BOP in polarized far-IR imaging. The angular resolution and surface brightness dynamic range of SALTUS–B-BOP will make it possible to resolve 0.1 pc-wide filaments out to $\sim 2\,\mathrm{kpc}$ and to image a few % polarized dust emission through the entire extent of nearby cloud complexes (cf. Fig. 1), from the low-density outer parts of molecular clouds ($A_V \sim 1$) all the way to the densest filaments and protostellar cores ($A_V > 100$). In comparison, *Planck* had far too low resolution in polarization ($10'$ at best) to probe the magnetic field within dense 0.1 pc-wide filaments or detect faint 0.1 pc-wide striations.

Ground-based or air-borne mm/submm polarimetric instruments, such as SCUBA2-POL, NIKA2-POL, SOFIA/HAWC+, or BLAST-TNG, will lack the required sensitivity and dynamic range in both spatial scales and intensity. BLAST-Pol operating at 250, 350, and 500 μm (Fissel et al., 2010), has only modest resolution ($30''$–$1'$), sensitivity, and dynamic range. HAWC+, the far-infrared camera and polarimeter for SOFIA (Dowell et al., 2010) and Super-BLAST-Pol, the next generation BLAST-Pol experiment (cf. Dober et al., 2014), both benefit from a large 2.5 m primary mirror and thus achieve a reasonably good angular resolution (a factor of 5–6 worse than SALTUS), but are two orders of magnitude less sensitive (NEP $> 10^{-16}\,\mathrm{W\,Hz^{-1/2}}$) than SALTUS–B-BOP. Future ground-based submm telescopes on high, dry sites such as CCAT-p and CSST will benefit from larger aperture sizes (6 m and 30 m, respectively) and will thus achieve an angular resolution comparable to SALTUS at 350 μm and 1 mm, respectively, but will be limited in sensitivity by the atmospheric background load on the detectors and in spatial dynamic range by the need to remove

atmospheric fluctuations.

Dust polarimetric imaging with ALMA at $\lambda \sim 0.8$–$3\,$mm provides excellent sensitivity and resolution, but only on small angular scales (from $\sim 0.02''$ to $\sim 1'$). Indeed, even with additional observations with the ACA compact array, the maximum angular scale recoverable by the ALMA interferometer remains smaller than $\sim 1'$ (see ALMA technical handbook)[1]. This implies that ALMA is intrinsically insensitive to all angular scales $> 1'$, corresponding to structures larger than 0.04–0.1 pc in nearby clouds. Using multi-configuration imaging, ALMA can achieve a spatial dynamic range of ~ 1000, comparable to that of *Herschel* or SALTUS–B-BOP, but only for relatively high surface brightness emission. Because ALMA can only image the sky at high resolution, it is indeed ~ 2–3 orders of magnitude less sensitive to low surface brightness emission than a single-dish space telescope such as SALTUS. Furthermore, the small size of the primary beam ($\sim 0.3'$-$1'$ at 0.8–3 mm) makes mosaicing of wide ($> 1\,\mathrm{deg}^2$) fields impractical and prohibitive with ALMA. In practice, ALMA polarimetric studies of star-forming molecular clouds will provide invaluable insight into the role of magnetic fields within individual protostellar cores/disks and will be very complementary to, but will not compete with, the SALTUS–B-BOP observations discussed here which target the role of magnetic fields on larger scales.

References

André, P., Arzoumanian, D., Könyves, V., Shimajiri, Y., & Palmeirim, P. 2019, A&A, 629, L4

André, P., Di Francesco, J., Ward-Thompson, D., et al. 2014, in Protostars and Planets VI, ed. H. Beuther et al., 27

André, P., Men'shchikov, A., Bontemps, S., et al. 2010, A&A, 518, L102

Arzoumanian, D., André, P., Didelon, P., et al. 2011, A&A, 529, L6

Arzoumanian, D., André, P., Könyves, V., et al. 2019, A&A, 621, A42

Arzoumanian, D., André, P., Peretto, N., & Könyves, V. 2013, A&A, 553, A119

Beck, R. 2015, A&A Rev., 24, 4

Bracco, A., Palmeirim, P., André, P., et al. 2017, A&A, 604, A52

Busquet, G., Estalella, R., Palau, A., et al. 2016, ApJ, 819, 139

Busquet, G., Zhang, Q., Palau, A., et al. 2013, ApJ, 764, L26

Ching, T.-C., Lai, S.-P., Zhang, Q., et al. 2017, ApJ, 838, 121

Cox, N. L. J., Arzoumanian, D., André, P., et al. 2016, A&A, 590, A110

Dall'Olio, D., Vlemmings, W. H. T., Persson, M. V., et al. 2019, A&A, 626, A36

Dober, B. J., Ade, P. A. R., Ashton, P., et al. 2014, in Proc. SPIE, Vol. 9153, Millimeter, Submillimeter, and Far-Infrared Detectors and Instrumentation for Astronomy VII, 91530H

Dowell, C. D., Cook, B. T., Harper, D. A., et al. 2010, in Proc. SPIE, Vol. 7735, Ground-based and Airborne Instrumentation for Astronomy III, 77356H

Fissel, L. M., Ade, P. A. R., Angilè, F. E., et al. 2010, in Proc. SPIE, Vol. 7741, Millimeter, Submillimeter, and Far-Infrared Detectors and Instrumentation for Astronomy V, 77410E–77410E–14

Galametz, M., Maury, A., Girart, J. M., et al. 2020, A&A, 644, A47

[1]Note that total power ALMA data can only be obtained for spectral line observations and are not possible in continuum.

Galametz, M., Maury, A., Girart, J. M., et al. 2018, A&A, 616, A139

Galametz, M., Maury, A. J., Valdivia, V., et al. 2019, A&A, 632, A5

Girart, J. M., Frau, P., Zhang, Q., et al. 2013, ApJ, 772, 69

Girart, J. M., Rao, R., & Marrone, D. P. 2006, Science, 313, 812

Guillet, V., Girart, J. M., Maury, A. J., & Alves, F. O. 2020, A&A, 634, L15

Hacar, A., Tafalla, M., Kauffmann, J., & Kovács, A. 2013, A&A, 554, A55

Hennebelle, P. & André, P. 2013, A&A, 560, A68

Hill, T., Motte, F., Didelon, P., et al. 2011, A&A, 533, A94

Hull, C. L. H., Mocz, P., Burkhart, B., et al. 2017, ApJ, 842, L9

Inoue, T., Hennebelle, P., Fukui, Y., et al. 2018, PASJ, 70, S53

Inoue, T. & Inutsuka, S.-i. 2012, ApJ, 759, 35

Inutsuka, S.-i., Inoue, T., Iwasaki, K., & Hosokawa, T. 2015, A&A, 580, A49

Inutsuka, S.-I. & Miyama, S. M. 1992, ApJ, 388, 392

Inutsuka, S.-I. & Miyama, S. M. 1997, ApJ, 480, 681

Kainulainen, J., Stutz, A. M., Stanke, T., et al. 2017, A&A, 600, A141

Könyves, V., André, P., Men'shchikov, A., et al. 2015, A&A, 584, A91

Kwon, W., Stephens, I. W., Tobin, J. J., et al. 2019, ApJ, 879, 25

Lada, C. J., Forbrich, J., Lombardi, M., & Alves, J. F. 2012, ApJ, 745, 190

Lee, Y.-N., Hennebelle, P., & Chabrier, G. 2017, ApJ, 847, 114

Li, Z.-Y., Banerjee, R., Pudritz, R. E., et al. 2014, in Protostars and Planets VI, ed. H. Beuther et al., 173

Marsh, K. A., Kirk, J. M., André, P., et al. 2016, MNRAS, 459, 342

Maury, A. J., Girart, J. M., Zhang, Q., et al. 2018, MNRAS, 477, 2760

Men'shchikov, A. 2013, A&A, 560, A63

Misugi, Y., Inutsuka, S.-i., & Arzoumanian, D. 2019, ApJ, 881, 11

Molinari, S., Swinyard, B., Bally, J., et al. 2010, A&A, 518, L100

Motte, F., Zavagno, A., Bontemps, S., et al. 2010, A&A, 518, L77

Nakamura, F., Hanawa, T., & Nakano, T. 1993, PASJ, 45, 551

Palmeirim, P., André, P., Kirk, J., et al. 2013, A&A, 550, A38

Planck int. res. XXXII. 2016, A&A, 586, A135

Planck int. res. XXXIII. 2016, A&A, 586, A136

Planck int. res. XXXV. 2016, A&A, 586, A138

Pudritz, R. E. & Kevlahan, N. K.-R. 2013, Philos. Trans. R. Soc. Ser. A, 371, 20248

Rieder, M. & Teyssier, R. 2017, MNRAS, 471, 2674

Schisano, E., Rygl, K. L. J., Molinari, S., et al. 2014, ApJ, 791, 27

Segura-Cox, D. M., Looney, L. W., Tobin, J. J., et al. 2018, ApJ, 866, 161

Seifried, D. & Walch, S. 2015, MNRAS, 452, 2410

Shimajiri, Y., André, P., Braine, J., et al. 2017, A&A, 604, A74

Tafalla, M. & Hacar, A. 2015, A&A, 574, A104

Valdivia, V., Maury, A., Brauer, R., et al. 2019, MNRAS, 488, 4897

Verliat, A., Hennebelle, P., Maury, A. J., & Gaudel, M. 2020, A&A, 635, A130

Yen, H.-W., Koch, P. M., Hull, C. L. H., et al. 2021, ApJ, 907, 33